Source multiplexing enhances the number of channels of a multispectral sensor

Maria Katsafadou, *Member, EMBS*, and Mario E. Giardini, *Member, IEEE*

***Abstract*— This paper presents preliminary work on a method to increase the number of detection channels of a commercial 6-channel spectrometric sensor, by employing a set of multiplexed spectrally colored illumination sources. A demonstrator has been built and tested on a set of independent dyes. The results suggest successful enhancement of the number of detection channels. More tests are needed to provide quantitative performance evaluation, and to demonstrate viability in a clinical setting.**

***Clinical Relevance*— The technique presented in this paper shows promise to provide a viable method for multispectral sensing in highly-miniaturized systems, such as in-vivo sensing capsules.**

I. Introduction

Endoscopic techniques are benefitting from a rapid evolution of miniaturised sensing technologies, to be deployed on board of in-body sensing capsules. Amongst these, optical spectroscopic and colorimetric sensing play a key role [1].

As a representative example, in our work we are interested in the detection of upper gastrointestinal tract bleeding (UGIB), one of the most common and serious complications of gastrointestinal diseases and/or surgery affecting approximately 70,000 people each year in the UK and 300,000 in the USA [2, 3].

Early bleeding detection is key to favorable clinical outcome, since any delay in diagnosis and intervention may lead to significant loss of blood and increases the patient's mortality risk [2, 4]. For example, in patients with ulcers, the most common cause of UGIB, acute bleeding stops by the time the person reaches the hospital in 90% of cases. However, if appropriate treatment is not given to the patient, life-threatening bleeding will re-occur in 30-50% of them [5].

The most recent evolutions in UGIB detection use telemetric capsule-based differential optical sensing at two wavelengths [2], that can be either swallowed for active bleeding detection, or anchored to the gastrointestinal wall for rebleeding detection. The sensitivity is high, albeit the specificity could benefit from an increase in the number of wavelengths, moving towards a multispectral/spectroscopic system.

Yet, commercial wavelength-resolved sensors for capsule sensing, either exhibit a low number of wavelengths, 10 being the practical maximum for a single compact device [6], or rely on bulky external spectrometers [7]. Ideally, we would want a spectrometric detector that is small enough while at the same time exhibiting a high number of optical detection bands.

This paper presents preliminary tests to increase the number of spectral bands sensed by a commercial multispectral sensor, by employing a set of time-multiplexed light sources with a dominant wavelength, thus shifting the peak sensitivity of each sensor channel. A simple set-up is described and tested on a set of multiple dye solutions.

II. Methodology

The experimental set-up is described in the following Section A. Then, in Section B, the description of the procedure followed to test the set-up is presented. In the last section, the data analysis is briefly explained.

A. Experimental Set-up

The experimental set-up is illustrated in Fig. 1. Four LEDs with different wavelengths are coupled into a 4cm integrating sphere. More specifically a 465 nm (blue, NSPB510AS, Nichia Corp., Japan), a 525 nm (green, NSPG500DS, Nichia Corp., Japan), a 600 nm (amber, NSPA510BS, Nichia Corp., Japan) and a white (GW QSSPA1.EM, Osram Licht AG, Germany) LEDs have been used. These LEDs are connected with load resistors of 680 Ohm to the 5V digital outputs of an Arduino MEGA board (Arduino S.r.l., Italy), yielding drive currents of approximately 4mA. The output voltage capabilities of the Arduino are above the threshold voltages for all these LEDs.

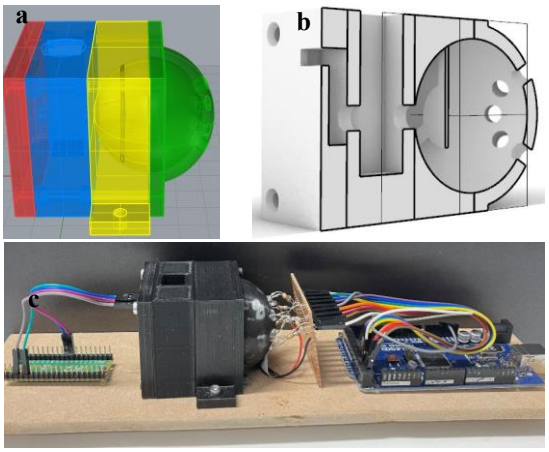

Figure 1. Schematic of experimental Set-up, a: CAD Design, b: Cross Section of Design, c: Photograph of the set-up

*Research supported by Medical Research Scotland, UK, and Ovesco Endoscopy AG (Grant Ref PhD-1048-2016).

M. Katsafadou and M. E. Giardini are with the Department of Biomedical Engineering, University of Strathclyde, Glasgow G1 1XQ, UK (e-mail: maria.katsafadou@strath.ac.uk).

An Arduino code has been written to power and control these LEDs, implementing time-multiplexing of the sources. Their light is scattered inside a 3D-printed integrating sphere with 40mm diameter, brush-coated with titanium white (Winsor & Newton Professional Acrylic PW6), mounted in the sphere in 5mm input ports. The sphere has a 6mm output port, protected from the LED line of sight by a baffle. The ratio between total port surface and total sphere surface is 3.6%. The output port is proximity-coupled to a cuvette, in turn proximity-coupled to a 6-channel AMS AS7262 color sensor (ams-OSRAM AG, Austria), that measures the transmitted light intensity at 6 spectral bands. The sensor output is pre-calibrated by the manufacturer for linearity and offset. More specifically, the six visible channels are able to detect with spectral sensitivity centered at 450nm (Violet), 500nm (Blue), 550nm (Green), 570nm (Yellow), 600nm (Orange) and 650nm (Red), each band with bandwidth at half-maximum of approximately 40nm.

The system has been 3D-printed on a Creality Ender 3 Pro FDM printer (Creality, China) using a PLA/PHA blend (colorFabb B.V., The Netherlands). A photograph of the system is presented in Fig. 1c.

The sensor communicates through a 3.3V I2C interface, and, therefore, communication with this sensor is achieved using a Raspberry Pi Pico (Raspberry Pi Foundation, UK) board, which operates at 3.3V. This is substantially simpler than e.g., using a logic level converter on a single control board. The Pico microcontroller is programmed in the Python programming language, to control and power the sensor, multiplexing with a 1s warm-up time for each source, and a 10ms integration time.

By time-multiplexing each LED, each spectral channel of the detector reads three signals, associated with the three individual LED sources. The spectral region investigated by each LED-channel pair is effectively given by the product of the source spectrum and the channel spectral sensitivity. In practice, therefore, with this multiplexing, each detector channel can detect three independent spectral regions. For each LED and detector channel, we therefore reconstructed from the datasheets the nominal spectral emissivity and sensitivity respectively, quantitatively retrieved from the datasheets using the WebPlotDigitizer utility [8], and performed the products. The 18 resulting products between source spectra and detector sensitivities are plotted in Fig. 2, alongside a table of the peak wavelengths for readability.

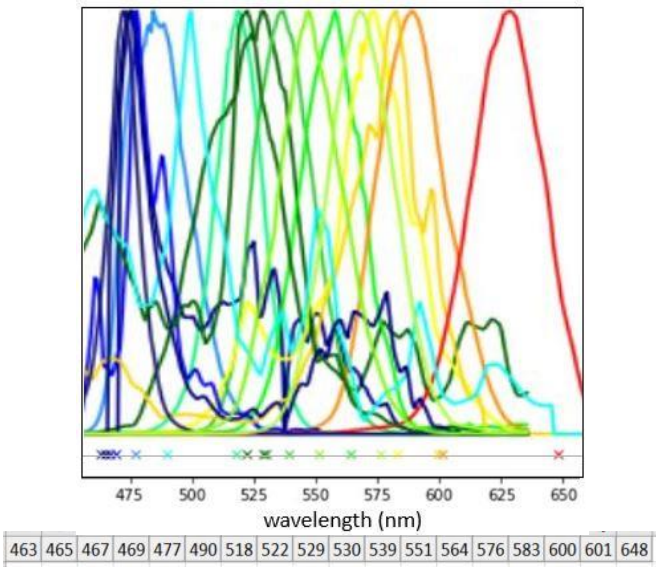

Figure 2. Normalized product between source spectra and detector sensitivity spectra, peak positions, and table of the peak wavelengths in nm.

B. *Sample Preparation*

In order to test the set-up, a set of 18 samples with independent spectra have been prepared. A set of 18 aqueous solutions of pure pigment solid watercolor paints (Winsor & Newton Artist's Professional Watercolors), which we assume having linearly independent spectra as traditionally used in painting, and not possible to emulate by mutual mixing, have been prepared at concentration of 0.05%. The identificatory names of these color dyes are presented in Table 1.

TABLE I. SAMPLE PIGMENTS

1.	Winsor yellow
2.	Lemon yellow
3.	Trans yellow
4.	Winsor orange
5.	Winsor red
6.	Alizarin crimson
7.	Permanent rose
8.	Winsor violet
9.	Winsor blue
10.	French ultramarine
11.	Indanthrene blue
12.	Permanent sap green
13.	Winsor green
14.	Raw umber
15.	Burnt umber
16.	Indigo
17.	Payne's gray
18.	Ivory black

More specifically, 5mg of each color, in the raw solid format, had been added to 50ml of distilled water. Then, the samples had been stirred for 5 minutes at room temperature using a magnetic stirrer. Following the stirring, the solutions have been stored in dark glass jars to protect them from fading due to long-term light exposure. Out of this master solution, a 5ml fraction has been further processed for measurement and to avoid scattering of the light due to particulate, the samples have then been filtered through polyethresulfone membrane filters with polypropylene housing, with pore size 0.45μm (UK-PES25, AllPure Biotechnology, UK) in combination with Terumo 2.5ml luer-lock syringes. The filtered samples have been stored in sterile cups.

To measure the samples absorbance, 4ml square plastic cuvettes with a 10mm light path and four clear sides have been used, covered with a lid to avoid sample contamination and evaporation (Fig. 3). In order to calculate the standard deviation and noise level of our measurements, each cuvette has been rotated clockwise in order to have measurements from each of the 4 directions available from the cuvette.

Figure 3. Prepared filtered samples.

Signals were measured for each sample from the 18 source-detector pairs, and the related absorbance A has been computed as defined in (1)

$$A = \log_{10} \frac{I_0}{I}. \quad (1)$$

where I_0 is the intensity of the light passing through a reference cell filled with distilled water, and I is the intensity of light passing through the sample.

C. Data Analysis

If the individual source-detector channel pairs indeed measure independent information, we expect the measured absorbance sequences of 18 data points from the 18 samples to be linearly independent. In order to verify this, we arranged the sequences in an 18x18 matrix, and calculated the eigenvalues using Matlab 2022a (The Mathworks, USA). The number of independent spectra is thus given by the number of non-zero eigenvalues (matrix rank), to be corrected for the small noise contribution from the data, as per the discussion below.

III. Results

The measured absorbance matrix, ordered by peak detection wavelengths numbered as in Fig. 2 (columns) and sample numbers as in Table 1 (rows) is reported in Table 2. The noise levels, as derived from the four measurements per sample, are below the limit of detection for most points, and reach a maximum of 0.5% of the mean spectral value.

The matrix eigenvalue modulus vector, ordered by magnitude, is reported in Table 3.

IV. Discussion

In the absence of noise, it is expected that the number of independent multispectral vectors ("spectra") will be equal with the rank of the 18x18 absorbance matrix. However, in any physical measurement, noise is inevitably present, albeit small such as in our measurements, and it is independent from channel to channel. Therefore, the calculation of the rank of the matrix is not indicative of linear independence, as the noise cancels any deviation from linear dependence of each spectrum. Indeed, in our case, the matrix rank is 18, indicating that the 18 spectra are not linearly dependent, while we observe that, in the available wavelengths, at least two pairs (529 and 530 nm, 600 and 601 nm) virtually coincide. This limits the practical number of independent spectra to, at most, 16. This is the reason the eigenvalues, rather than the rank, have been calculated individually.

In general, the problem of estimating eigenvalues in the presence of an additive random noise is a non-trivial problem [9], well beyond the scope of this paper. In practical terms, however the eigenvalue modulus remains above the order of magnitude of the noise level for a number of eigenvalues equal to the number of independent spectra, and the first eigenvalue is higher compared to the rest [9]. This corresponds to our table III, with the first eigenvalue close to 4, and the next 12 in close proximity with each other. In the eigenvalue sequence in Table 2 the eigenvalues do not significantly drop until after the 13th value, indicating that the signal sequences for at least 13 source-detector channel pairs are linearly independent with each other.

TABLE II. Absorbance Matrix

0.544	0.772	0.556	0.592	0.916	0.342	0.302	0.544	0.301	0.544	0.579	0.439	0.426	0.269	0.443	0.444	0.400	0.397
0.447	0.530	0.515	0.509	0.535	0.497	0.500	0.544	0.602	0.544	0.559	0.564	0.574	0.554	0.506	0.542	0.520	0.560
0.368	0.555	0.345	0.322	1.501	0.064	0.049	0.211	0.090	0.354	0.152	0.087	0.125	0.036	0.104	0.092	0.076	0.071
0.243	0.345	0.278	0.262	0.372	0.152	0.087	0.301	0.067	0.243	0.278	0.196	0.146	0.069	0.211	0.198	0.134	0.126
0.669	0.651	0.653	0.720	0.601	0.740	0.626	0.669	0.602	0.512	0.728	0.643	0.699	0.488	0.728	0.806	0.828	0.871
0.192	0.247	0.278	0.262	0.225	0.196	0.106	0.269	0.163	0.192	0.306	0.196	0.247	0.081	0.339	0.342	0.348	0.284
0.146	0.230	0.283	0.243	0.167	0.196	0.088	0.336	0.125	0.114	0.408	0.263	0.234	0.056	0.426	0.412	0.375	0.248
0.368	0.304	0.477	0.447	0.171	0.865	0.668	0.637	0.426	0.269	0.942	0.740	0.699	0.388	1.198	1.184	1.089	0.954
0.243	0.049	0.141	0.208	0.057	0.497	0.934	0.146	0.602	0.211	0.074	0.263	0.316	0.860	0.189	0.303	0.495	0.682
0.192	0.182	0.195	0.208	0.192	0.228	0.296	0.243	0.275	0.211	0.213	0.246	0.275	0.296	0.213	0.241	0.280	0.302
0.447	0.249	0.368	0.419	0.219	0.831	1.112	0.447	0.845	0.415	0.394	0.564	0.544	1.015	0.553	0.662	0.773	0.916
0.301	0.311	0.255	0.262	0.362	0.196	0.294	0.243	0.243	0.336	0.249	0.263	0.243	0.438	0.194	0.202	0.208	0.230
0.447	0.238	0.255	0.306	0.353	0.439	0.923	0.204	0.660	0.544	0.168	0.342	0.331	1.286	0.172	0.227	0.287	0.429
0.192	0.243	0.199	0.196	0.270	0.112	0.108	0.160	0.125	0.172	0.199	0.138	0.145	0.104	0.156	0.156	0.140	0.138
0.669	1.179	0.836	0.763	1.384	0.439	0.356	0.813	0.391	0.637	0.866	0.564	0.574	0.313	0.653	0.586	0.502	0.471
0.669	0.463	0.602	0.669	0.452	1.041	1.639	0.637	0.845	0.637	0.579	0.740	0.813	1.150	0.772	0.958	1.233	1.513
0.572	0.438	0.515	0.582	0.431	0.865	1.017	0.512	0.778	0.512	0.502	0.564	0.637	0.762	0.603	0.712	0.845	0.969
0.257	0.288	0.265	0.276	0.300	0.228	0.155	0.269	0.079	0.254	0.279	0.263	0.176	0.152	0.256	0.261	0.177	0.178

Rows: dyes, columns: wavelengths, sequence as per Fig.2 and Table 2

TABLE III. Eigenvalues of the absorbance matrix.

3.8990	0.3432	0.3432	0.1257	0.1079	0.0974	0.0974	0.0772	0.0772	0.0729	0.0729	0.0476	0.0476	0.0281	0.0281	0.0220	0.0220	0.0037

These results are consistent with Fig. 2. There, we have 18 independent peaks. However, as already noted, some of the values are at close proximity with each other, moreover with the uncertainty, difficult to estimate quantitatively and reliably, associated with the reconstruction of the peak shape from nominal datasheet plots. 13 isolated wavelength peaks or peak clusters are clearly identifiable.

Further investigation is needed to confirm our initial idea. From the point of view of purely nominal performance, the number of attainable linearly independent detection channels needs to be determined more reliably. This will entail a systematic measurement of spectral emissivity from the sources, of spectral sensitivity of the detector channels, and of the linear compliance and offset of the detector calibration provided by the manufacturer. This data needs to be measured directly, rather than relying on reverse reconstruction from plots on manufacturer datasheets. Additionally, a set of test samples with better control of the chemical composition will need to be designed and employed.

More importantly, the value of the approach in endoscopic capsule sensing will need to be demonstrated on a scenario of clinical relevance, e.g., blood and/or bile detection in the presence of heavy contaminants, determination of blood oxygen content, or similar problems of relevance to optical spectrometric/colorimetric sensing.

In any case, however, even with the simple demonstrator used in our study, the results are suggestive that indeed, the number of independent multispectral channels has been augmented using multiplexed spectrally colored sources.

ACKNOWLEDGMENT

We wish to thank Sebastian Schostek and Henrik Buchelet, of Ovesco Endoscopy AG, for useful discussion.

REFERENCES

[1] Z. He, P. Wang and X. Ye, "Novel endoscopic optical diagnostic technologies in medical trial research: recent advancements and future prospects", BioMedical Engineering OnLine, vol. 20, no. 1, 2021. Available: 10.1186/s12938-020-00845-5.

[2] S. Schostek, M. Zimmermann, J. Keller et al., “Telemetric real-time sensor for the detection of acute upper gastrointestinal bleeding”, Biosensors and Bioelectronics, 78 (2016), pp. 524–529.

[3] G. Zuckerman, C. Prakash, “Acute lower intestinal bleeding Part I: Clinical presentation and diagnosis”, Gastrointestinal Endoscopy, 48(6), 1998, pp.606-616.

[4] C. Van de Bruaene, D. De Looze, P. Hindryckx, “Small bowel capsule endoscopy: Where are we after almost 15 years of use”, World Journal of Gastrointestinal Endoscopy, 7(1), 2015, pp. 13-36.

[5] J. Sung, E. Kuipers, A. Barkun, “Gastrointestinal Bleeding”, 2012 Wiley-Blackwell.

[6] Adafruit Industries, “Adafruit AS7341 10-Channel Light / Color Sensor Breakout”, Created by Bryan Siepert, Last Updated: 30-Oct-2020.

[7] K. Ehrlich, A. Kufcsák, N. Krstajić, R. K. Henderson, R. R. Thomson, M. G. Tanner, "Fibre optic time-resolved spectroscopy using CMOS-SPAD arrays," Proc. SPIE 10058, Optical Fibers and Sensors for Medical Diagnostics and Treatment Applications XVII, 100580H (28 February 2017); https://doi.org/10.1117/12.2252090

[8] "WebPlotDigitizer - Copyright 2010-2021 Ankit Rohatgi", Apps.automeris.io, 2022. [Online]. Available: https://apps.automeris.io/wpd/. [Accessed: 21- Jan- 2022].

[9] A. Edelmann, “Eigenvalues and Condition Numbers of Random Matrices”, PhD Thesis (Mathematics),1984, Yale